PHYSICAL REVIEW A **84**, 020301(R) (2011)

Generation and homodyne detection of continuous-variable entangled optical beams with a large wavelength difference

Xiaomin Guo (郭晓敏), Changde Xie (谢常德), and Yongmin Li (李永民)*
State Key Laboratory of Quantum Optics and Quantum Optics Devices, Institute of Opto-Electronics, Shanxi University, Taiyuan 030006, China
(Received 20 May 2011; published 2 August 2011)

We present a scheme for generating and homodyne detecting of continuous-variable entanglement of bright optical beams with a large wavelength difference by utilizing an optical parametric oscillator (OPO) and an optical parametric amplifier (OPA) simultaneously. Entangled optical beams at 0.8 and 1.5 μm are generated from the OPA; the seed beams injected in the OPA as well as the local oscillators at the two wavelengths needed for homodyne detection are provided by the OPO. The entangler is a ring resonator involving a second-order nonlinear crystal that is pumped from two opposite directions. In one direction the pump power is above the oscillation threshold and the optical nonlinear resonator operates as an OPO. In the other direction the pump power is below the threshold and it operates as a phase-sensitive frequency nondegenerate optical parametric amplifier. Our scheme combines the advantages of both OPO and OPA quantum optical devices and opens another avenue for preparation and homodyne detection of high quality bright entangled light with a large wavelength difference.

DOI: 10.1103/PhysRevA.84.020301 PACS number(s): 03.67.Mn, 42.50.Dv, 42.65.Yj

Entanglement is one of the most important resources for quantum information processing [1] and has its roots in many key discoveries of quantum information science in the past two decades [2–5], including quantum key distribution, quantum dense coding, quantum teleportation, quantum repeater, quantum computation, and quantum metrology, etc. For the physical implementation of a future quantum network [6], the quantum information needs to be transferred with high fidelity between the nodes which consist of different physical systems (usually with different characteristic frequencies) [7–11]; quantum teleportation is a strong candidate to achieve such tasks [12,13]. To realize a high fidelity teleportation between the nodes with different characteristic frequencies, the entangled beams used for transporting quantum information must have different frequencies and a high degree of entanglement. In optical continuous-variable (CV) quantum information protocols, entangled states with balanced quantum correlations in both amplitude and phase quadratures are desired. For instance, in quantum key distribution it improves the security and in quantum teleportation, the errors introduced by imperfections are equally distributed among the quadratures of the teleported state.

The intracavity second-order nonlinear process is an efficient method to generate CV entanglement. Entangled states with a small frequency difference (740 MHz) have been demonstrated with a nondegenerate optical parametric amplifier (OPA) [14]. However, in this experiment the injected signal of OPA and the local oscillator (LO) for the homodyne detection are derived from the fundamental pump laser; because of this intrinsic limitation, only a frequency near-degenerate entangled state can be prepared and homodyne detected. On the other hand, sophisticated electro-optic modulation systems are required in this protocol [14]. By employing a depleted optical parametric amplifier, entanglement of fundamental and second-harmonic fields was also observed [15], in which the frequencies of the entangled light are strictly limited to the fundamental and harmonic frequencies.

An optical parametric oscillator (OPO) above the threshold can generate intense optical beams with CV quantum entanglement and tunable frequencies [16]. Two-color [17–20] and three-color [21] CV entangled states have been observed based on this scheme. In all these experiments the measured phase-quadrature correlations are much less than the corresponding amplitude-quadrature correlations. The imbalance between the amplitude and phase correlations partially derives from the additional phase noises due to the scattered light by thermal phonons [22]. On the other hand, the phase-sum noise of the twin beams from an OPO essentially depends on the pump power. The higher the pump power is, the larger the phase-sum noise is. Only when the pump power reaches the threshold of the OPO could the phase correlation be the same as the amplitude correlation [23]. In order to obtain good balance between the phase and amplitude correlations, the OPO has to be operated at a pump level very close to its threshold (for example, a few percent above the threshold), and unfortunately the OPO is very unstable in this case [17]. To date, the preparation of two-color CV entanglement with any optical frequencies and balanced squeezing in both quadratures which are crucial to the quantum information is still a challenge.

In general, frequency nondegenerate OPOs operating at two different conditions (above or below the oscillation threshold) have different characteristics. Above the threshold (the OPO), frequency tunable and intense entangled twin beams can be generated and directly measured [17,18], but the quantum correlation of phase sum is limited by the practical operation conditions and it is difficult to balance the quantum correlations of the phase sum and the amplitude difference. Below the threshold (the OPA), it can provide highly squeezed and balanced two-mode entangled states, but does not allow a practical homodyne measurement of the quantum state due to

*Corresponding author: yongmin@sxu.edu.cn; liyongminwj@163.com

the absence of appropriate LO. In this rapid communication, we present a device (the entangler) which joins the best characteristics of the OPO and OPA, and can generate highly tunable CV entangled beams with a large wavelength difference and balanced squeezing. The entangler is a ring nonlinear resonator pumped from two opposite directions, where the pump powers in the forward and backward directions are above and below the threshold, respectively. The intense signal and idler produced by the forward OPO are used for the injected signals of the backward OPA and the LO of the homodyne detection, and the entangled states are produced from the backward OPA. Using the OPO and OPA system the CV entanglement with almost balanced amplitude-difference and phase-sum quantum correlations were experimentally achieved and the quantum correlations between the signal at 0.8 μm and the idler at 1.5 μm are measured by the usual means of homodyne detection. The presented work provides a scheme for preparing and homodyne detecting highly tunable CV optical entangled states with high and balanced squeezing in both quadratures.

Figure 1 shows the schematic diagram of the experimental setup. The laser source is a homemade 526.5-nm single-frequency continuous wave Nd:YLF/KTP laser which can deliver single frequency output power of 500 mW. A Faraday isolator was set in the input light of the OPO and OPA to eliminate the back-reflection. A beam splitter was used to split the pump beam into two parts which pump the OPO and OPA in two opposite directions, respectively. The ring optical cavity is in a bow tie configuration consisting of two concave mirrors with 60-mm radii of curvature and two plane mirrors. The waist of the pump beam is ~50 μm inside the nonlinear crystal. The two input couplers were coated for high reflectivity at 0.8 and 1.5 μm (>99.8%) and high transmission at 526.5 nm (98%). The output coupler was coated for high reflectivity at 526.5 nm (>99%) and partial transmission (~6%) at 0.8 and 1.5 μm. The rest of the plane mirror was coated for high reflectivity at 526.5 nm (>99%), 0.8 μm, and 1.5 μm (>99.8%). A 20-mm-long periodically poled $KTiOPO_4$ (PPKTP) with both end faces antireflection coated at 0.53, 0.8, and 1.5 μm were used as the nonlinear medium. The temperature of the crystal oven was set to 25 °C and the measured wavelengths of the signal and idler beams were 808 and 1511 nm, respectively. Taking into account the optical path length of the OPO and OPA cavity (312 mm) and the intracavity linear loss of 1.7%, the free spectral range and the linewidth of the cavity are calculated to be ~960 and 11.8 MHz, respectively.

A stable ring resonator allows for the simultaneous resonance of two independent linearly polarized transverse electromagnetic fundamental modes (TEM_{00}) with opposite propagation directions. For a ring resonator-based doubly resonant OPO and OPA, the forward and backward TEM_{00} modes will experience exactly the same path, which means both modes have the same linear and nonlinear losses, phase shift, phase-matched conditions, etc. When pumped bidirectionally, the forward OPO and backward OPA both oscillate on a signal-idler mode pair and these two mode pairs have the same frequencies. In the experiment, when the output signal (idler) beams from the two directions were combined at a 50 : 50 beam splitter and the phase of one of the beams was scanned, high visibility fringes were clearly observed which confirmed the consistency of the forward and backward propagating TEM_{00} modes. The main part of the intense signal and idler beams at 0.8 and 1.5 μm emitting from the OPO served as the LOs which were needed by the homodyne detector. The rest was attenuated by a neutral density filter (NDF) and then injected into the OPA to act as the seed field.

Figure 2 shows the classical parametric amplification and deamplification observed when the relative phase between the pump and seed fields was scanned, which clearly shows that the frequency nondegenerate OPA is phase sensitive. To observe the entanglement, the OPO and OPA cavity was held on resonance with the signal-idler mode pair via a dither-locking method. At the same time, the relative phase was fixed by a servo loop in order to achieve the maximum parametric amplification. The pump power was set to be 1.22 times the threshold power in the forward direction (the generated down-converted field was 29 mW) and 0.72 times the threshold power in the backward direction. The main part of the signal and idler fields were separated by a dichroic beam splitter (DBS) and each beam was then directed to a 50 : 50 beam splitter to serve as a LO, while a small portion of them

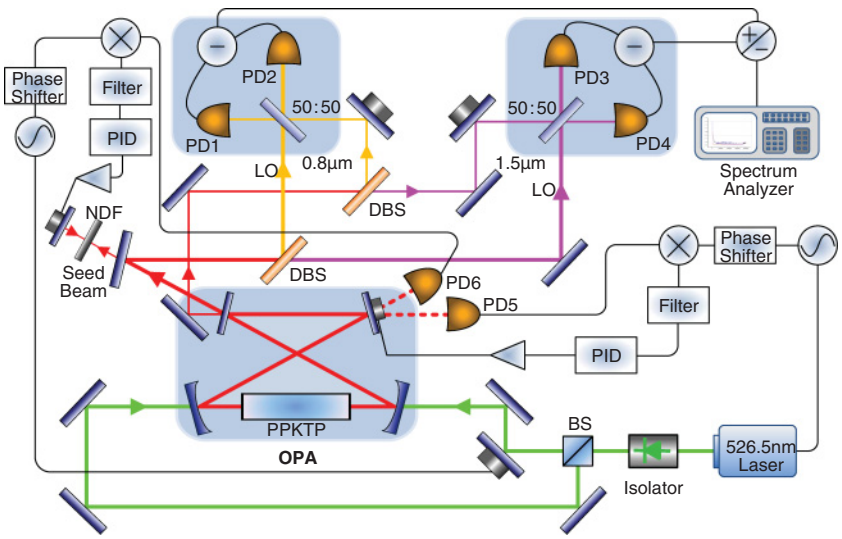

FIG. 1. (Color online) Schematic of the experimental setup. BS: beam splitter; DBS: dichroic beam splitter; PD: photodiode; PID: proportional-integral-derivative controller; LO: local oscillator; NDF: neutral density filter.

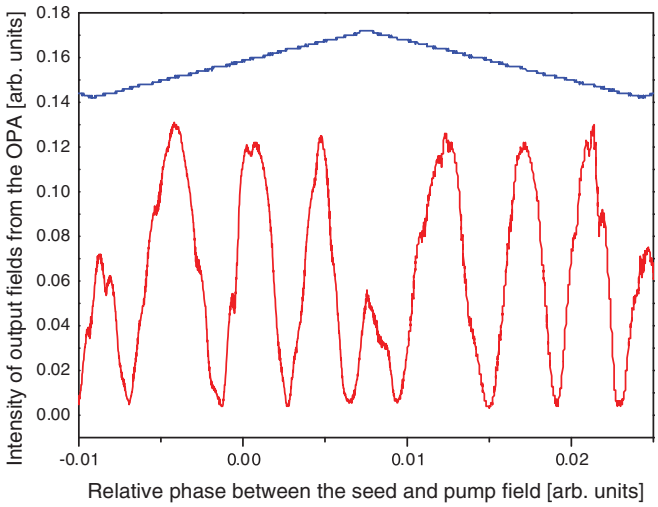

FIG. 2. (Color online) Observation of classical parametric amplification and deamplification when the relative phase between the seed and pump fields was scanned by using a triangle wave voltage signal.

(4.7 μW) was injected into the OPA to be the seed field. The observation of quantum entanglement was performed by means of two balanced homodyne detectors, which were built from two ETX-500 (Epitaxx) and two FND-100Q (EG&G) photodiodes, respectively. The measured quantum efficiency is 83% and 75% for 1.5 μm and 0.8 μm, respectively. A fringe visibility of 95% between the signal beam and LO on the 50 : 50 beam splitter was achieved. The photocurrent signals were recorded using a spectrum analyzer.

Figure 3 presents the amplitude-quadrature difference noise spectrum of the entangled fields at 0.8 and 1.5 μm from the OPA. Trace (a) corresponds to the quantum noise limit (QNL) which was measured with the output of the OPA blocked. Trace (b) is the amplitude-quadrature difference noise

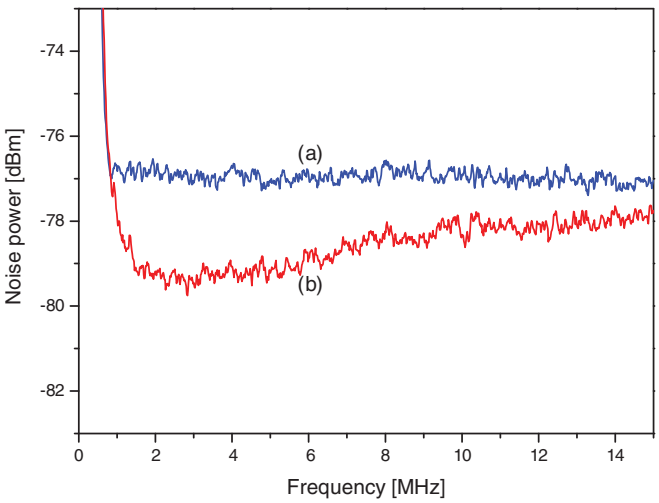

FIG. 3. (Color online) Amplitude-quadrature difference noise spectrum between the 0.8- and 1.5-μm optical fields; (a) quantum noise limit; (b) amplitude-quadrature difference noise spectra. The settings of the spectrum analyzer: Resolution bandwidth is 300 kHz and video bandwidth is 100 Hz.

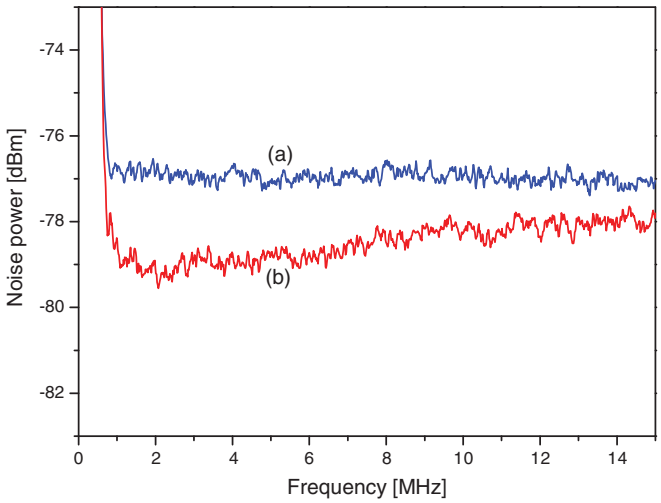

FIG. 4. (Color online) Phase-quadrature sum noise spectrum between the 0.8- and 1.5-μm optical fields; (a) quantum noise limit; (b) phase-quadrature sum noise spectra. The settings of the spectrum analyzer are the same as those in Fig. 3.

spectrum of the entangled fields which was measured with the LO phase fixed to the amplitude quadrature of each entangled beam. The observed amplitude-quadrature difference quantum correlation is 2.35 dB at 2.5 MHz. Figure 4 shows the phase-quadrature sum noise spectrum of the entangled fields from the OPA. Trace (a) corresponds to the QNL. Trace (b) is the phase-quadrature sum noise spectrum which was measured with the LO phase fixed to the phase quadrature of each entangled beam. The phase-quadrature sum quantum correlation of 2.25 dB was observed at 2.5 MHz. In Figs. 3 and 4, the electronic dark noise of the detectors which is ~9.5 dB below the QNL has been subtracted, and the QNL was also calibrated by a thermal white-light source.

The quantum entanglement between the 0.8- and 1.5-μm optical fields was verified according to the inseparability criterion [24], i.e., a violation of the inequality $\langle\Delta^2(\hat{X}_1 - \hat{X}_2)\rangle + \langle\Delta^2(\hat{Y}_1 + \hat{Y}_2)\rangle \geqslant 2$, where $\hat{X}_j$ and $\hat{Y}_j$ ($j = 1,2$) are amplitude and phase quadratures, respectively. Using the experimental values of $\langle\Delta^2(\hat{X}_1 - \hat{X}_2)\rangle = 0.582$ and $\langle\Delta^2(\hat{Y}_1 + \hat{Y}_2)\rangle = 0.595$, we have $\langle\Delta^2(\hat{X}_1 - \hat{X}_2)\rangle + \langle\Delta^2(\hat{Y}_1 + \hat{Y}_2)\rangle = 1.177 < 2$, which indicates the 0.8- and 1.5-μm optical fields from the OPA were indeed quantum entangled.

The observed entanglement in the current experimental system is limited by the nonperfect detection efficiency (including the quantum efficiency of the photodiodes and the optical propagation efficiency), the escape efficiency of the OPA, the fluctuations of the OPA cavity length, and the relative phases between the seed and pump fields, etc. These technical problems can be overcome in principle and a high degree of entanglement can be expected as shown recently in Refs. [25,26]. To make the system more versatile, it is desired that the system has good frequency tunability. By adjusting the crystal temperature and cavity length, the wavelengths of entangled beams can be coarsely tuned over several tens of nanometers (a larger tuning range is feasible if a multigrating PPKTP is employed), and continuous frequency tuning is also attainable by smooth tuning the pump laser [27].

In conclusion, we experimentally demonstrated the generation and the homodyne measurement of the entangled optical beams at 0.8- and 1.5-μm wavelengths using a dual-end-pumped nonlinear ring resonator. The presented protocol paves the way for preparing and detecting high quality two-color CV entanglement of a light field with any expected frequencies. The results presented will find promising applications in quantum information processing, such as the linking of two optical systems at different wavelengths. In particular, the currently demonstrated wavelengths of 0.8 and 1.5 μm will enable the transfer of CV quantum information between alkaline atoms and light fields of telecommunication wavelength.

This research is supported by the National Science Foundation of China (Grants No. 11074156 and No. 60736040), the TYAL, the National Key Basic Research Program of China (Grant No. 2010CB923101), the NSFC Project for Excellent Research Team (Grant No. 60821004), and the Research Project Supported by Shanxi Scholarship Council of China.

[1] R. Horodecki, Rev. Mod. Phys. **81**, 865 (2009).
[2] S. L. Braunstein and P. V. Loock, Rev. Mod. Phys. **77**, 513 (2005).
[3] N. Gisin and R. Thew, Nat. PhotonICS **1**, 165 (2007).
[4] T. D. Ladd, Nature (London) **464**, 45 (2010).
[5] V. Giovannetti *et al.*, Nat. Photonics **5**, 222 (2011).
[6] H. J. Kimble, Nature (London) **453**, 1023 (2008).
[7] B. Julsgaard *et al.*, Nature (London) **432**, 482 (2004).
[8] C. W. Chou *et al.*, Nature (London) **438**, 828 (2005).
[9] T. Chanelière *et al.*, Nature (London) **438**, 833 (2005).
[10] M. D. Eisaman *et al.*, Nature (London) **438**, 837 (2005).
[11] A. I. Lvovsky *et al.*, Nat. Photonics **3**, 706 (2009).
[12] C. H. Bennett, G. Brassard, C. Crépeau, R. Jozsa, A. Peres, and W. K. Wootters, Phys. Rev. Lett. **70**, 1895 (1993).
[13] A. Furusawa *et al.*, Nature (London) **282**, 706 (1998).
[14] C. Schori, J. L. Sorensen, and E. A. Polzik, Phys. Rev. A **66**, 033802 (2002).
[15] N. B. Grosse, S. Assad, M. Mehmet, R. Schnabel, T. Symul, and P. K. Lam, Phys. Rev. Lett. **100**, 243601 (2008).
[16] M. D. Reid and P. D. Drummond, Phys. Rev. Lett. **60**, 2731 (1988); M. D. Reid, Phys. Rev. A **40**, 913 (1989); P. D. Drummond and M. D. Reid, Phys. Rev. A **41**, 3930 (1990).
[17] A. S. Villar, L. S. Cruz, K. N. Cassemiro, M. Martinelli, and P. Nussenzveig, Phys. Rev. Lett. **95**, 243603 (2005).
[18] X. L. Su *et al.*, Opt. Lett. **31**, 1133 (2006).
[19] J. Jing, S. Feng, R. Bloomer, and O. Pfister, Phys. Rev. A **74**, 041804 (2006).
[20] Y. M. Li *et al.*, Appl. Phys. Lett. **97**, 031107 (2010).
[21] A. S. Coelho *et al.*, Science **326**, 823 (2009).
[22] J. E. S. César, A. S. Coelho, K. N. Cassemiro, A. S. Villar, M. Lassen, P. Nussenzveig, and M. Martinelli, Phys. Rev. A **79**, 063816 (2009).
[23] C. Fabre *et al.*, J. Phys. (Paris) **50**, 1209 (1989).
[24] L. M. Duan, G. Giedke, J. I. Cirac, and P. Zoller, Phys. Rev. Lett. **84**, 2722 (2000).
[25] M. Mehmet, H. Vahlbruch, N. Lastzka, K. Danzmann, and R. Schnabel, Phys. Rev. A **81**, 013814 (2010).
[26] Y. Wang *et al.*, Opt. Express **18**, 6149 (2010).
[27] C. C. Liu *et al.*, Appl. Opt. **50**, 1477 (2011).